J Geophys (1984) 55:23–30

Journal of Geophysics

On the identification of a transition zone in electrical conductivity between the lithosphere and asthenosphere: a plea for more precise phase data

Tony Cavaliere and Alan G. Jones *

Geophysics Laboratory, Physics Department, University of Toronto, Toronto, Ontario, Canada, M5S 1A7

Abstract. The magnetotelluric analytical solutions for an earth containing transitional layers in which the electrical conductivity is a function of depth has been considered previously for certain types of restricted models. However, an analytical formulation for an arbitrary n-layered earth containing both constant conductivity layers and transitional layers has not been published. Herein is presented a general matrix technique for such a problem in which the solution matrix is built up from $n-1$ layer connection matrices. The solution matrix is extremely sparse for n large and can be solved by $O(n)$ operations rather than the usual $O(n^3)$.

This theory is applied to generate the theoretical surface response two specific models of the lithosphere and asthenosphere. The first model has a lithosphere/asthenosphere boundary at 80 km and is representative of "young" oceanic crust and upper mantle. The other model is representative of a continental crust and upper mantle structure with an asthenosphere below 160 km depth.

For both models, techniques of linear inverse theory are applied to ascertain if a transitional zone between the lithosphere and asthenosphere could be resolved by surface measurements. It is shown that the impedance phase data is far more important for resolving this model parameter than is the apparent resistivity data. Accordingly, the need for more precise phase information is stressed.

Key words: ELAS project – Electrical lithosphere/asthenosphere structure – Magnetotelluric method – Baltic shield.

Introduction

The identification of an "electrical asthenosphere", or ELAS layer, beneath the oceanic and continental lithospheres is the subject of intense enquiry at present within the electromagnetic induction community. [The activities of the ELAS ad hoc committee of Working Group I/3 of IAGA (International Association of Geomagnetism and Aeronomy) are reported in the IAGA news publications (Vanyan, 1980; Schmucker, 1981; Schmucker, 1982).] By far the most considerable success has been achieved by ocean-bottom experiments that have detailed zones of high conductivity beneath both the Atlantic and Pacific oceanic lithospheres (Cox et el., 1980; Filloux, 1980a, b, 1981; Oldenburg, 1981; Chave et al., 1981). There is strong evidence in these data that the depth to these ELAS zones increases with increasing age of overlying oceanic crust.

On the continental lithosphere, Jones (1980, 1982a, b, 1984) and Jones et al. (1983) have presented models for various regions of northern Scandinavia that demand conducting zones beginning at depths in the range 110–200 km. Such zones, of increased conductivity, are also interpreted to begin at a depth of 70 km beneath the Kola peninsular (Kransnobaeva et al., 1981), at 50–80 km beneath the Pannonian basin (Ádám et al., 1982), at 100 km beneath the Grenville Province of the Canadian shield (Kurtz, 1982) and at 170 km beneath Tucson, Arizona (Larsen, 1977).

The majority of the above authors interpreted their estimated response functions in terms of one-dimensional (1D) layered-earth models (an example of such a model is illustrated in Fig. 1a). Many presented not only the "best-fitting" (defined in some manner) models, but also the range of possible models permitted by the statistical errors associated with the estimates. Whereas constant conductivity layered-earth models are perfectly satisfactory and justifiable for describing certain geological situations, e.g. sedimentary basins, it is to be expected that there exists a transition zone of finite width between the low electrical conductivity of the base of the lithosphere and the high conductivity of the ELAS zone. Hence, the question arises as to whether the parameterization of the earth's upper mantle into discrete layers is a satisfactory and adequate representation of the lithosphere/asthenosphere boundary.

Oldenburg (1981) and Kurtz (1982) have presented inversions of response functions in terms of models in which the conductivity varies continuously with depth (an example of this class of models is illustrated in Fig. 1b). These models can be thought of as the other alternative, in that the transition zone may be overemphasized and have too great a width.

In order to compromise between these two extremes

Offprint requests to: A.G. Jones

* *Present address:* Division of Seismology and Geomagnetism, Earth Physics Branch, Energy, Mines and Resources, 1 Observatory Crescent, Ottawa, Ontario, Canada K1A 0Y3

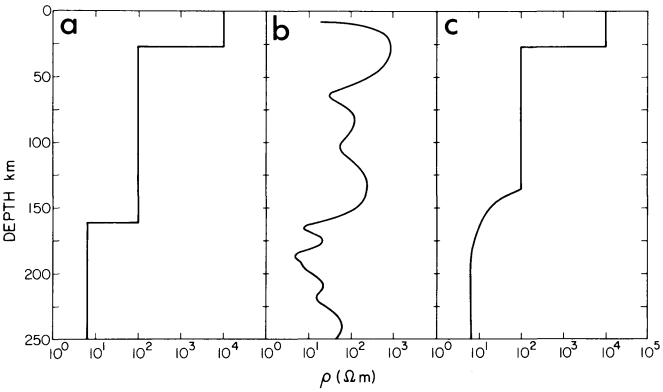

Fig. 1. Three classes of models of the earth which are acceptable to the Kiruna response (see Fig. 8). *a* Three-layered model with constant conductivity in each layer. *b* C^{2+} model with a continuous variation of conductivity with depth. *c* Four-layered model with a transition zone between the lower lithosphere and the asthenosphere

of model parameterization, we consider the case where there exists a transition zone, in which the conductivity varies linearly with depth, between two layers of constant conductivity (Fig. 1c illustrates an example of such a model). Kao (1981, 1982) and Kao and Rankin (1980) have considered this class of models and have presented the analytical formulation for the restricted case of a maximum of three layers, of which one may be a transition zone. They show that the electromagnetic fields within the transition zone layer may be expressed in terms of Airy functions of the first and second kinds. We have generalized their approach by considering an n-layer problem in which any or all of the layers can have a conductivity that varies linearly with depth. By matching the appropriate boundary conditions at the interfaces between the layers, of which four possible cases exist, we build up a complex sparse solution matrix. This solution matrix is then inverted to yield the complex impedance observed on the surface. The theory for this approach is presented in the following section.

To ascertain which of the parameters of a given model are resolvable, certain aspects of linearized inversion theory can be applied. Herein, the system matrix relating infinitesimally small variations of the model parameters to the resulting variations produced in the observed surface impedance is factored using a singular value decomposition (SVD). The SVD of the system matrix $\mathbf{A}$, which relates infinitesimally small order changes in the model parameters (Δp) to the changes thereby introduced in the response functions (Δc), by $\Delta c = \mathbf{A}\Delta p$, factorizes $\mathbf{A}$ into three matrices $\mathbf{A} = \mathbf{U}\Lambda\mathbf{V}^T$. These three are known as the matrix of singular values (Λ), the data eigenvector matrix ($\mathbf{U}$) and the parameter eigenvector matrix ($\mathbf{V}$). Such a factoring orders the model parameters, or combinations of model parameters, into one of three classes: either *important*, *marginally important*, or *unimportant*. The theory for this technique will not be presented as it is now a standard tool. [The reader is referred to, for example, Wiggins (1972), Lawson and Hanson (1974), Edwards et al. (1981), Jones (1982a) and Ilkisik and Jones (1984).] Also, the model parameter intercorrelations are computed and discussed (Lawson and Hanson, 1974; Inman, 1975).

In this work, we apply the theory presented in the following section, and the above-mentioned linearized inverse theory, to two specific models of a transition zone between the lower lithosphere and the upper asthenosphere. The first model is representative of a "young" oceanic environment, in which the depth to the ELAS layer is of the order of 80 km. The theoretically observed responses for such a model are calculated for the period range of observation of a typical natural source sea-floor electromagnetic experiment (0.1–10 cph), and standard errors are assigned to the responses. The second model is representative of the north-western part of the Baltic shield with an ELAS layer beginning at a depth of some 160 km. Variations in the possible thickness of a transition zone are considered by comparing the appropriate theoretical response function to actual field data.

For both of these studies, the importance of reliable phase estimates, with small associated standard errors, is shown. Although for a model in which the conductivity varies with depth alone the theoretically observed magnetotelluric (MT) apparent resistivity is related to the phase of the impedance by the Hilbert transform (see, for example, Weidelt, 1972; Fischer and Schnegg, 1980; Jones, 1980), in practice the variations in the gradient of the apparent resistivity are too subtle, given the errors in the data. Also, it is often the case that although the apparent resistivity data are well estimated, i.e. have small standard errors, the phase data are not so well estimated. This may be due to either timing problems (see, for example, Jones et al., 1983) or to inadequate techniques of statistical frequency analysis being applied to the data. Hence, the structure of the error at a particular frequency is not a circle in the complex impedance plane (Fig. 2a), but is more like the kidney shape of Fig. 2b. Accordingly, the aim of this paper is to emphasize the requirement for a greater effort to be expended in the more precise estimation of impedance phase.

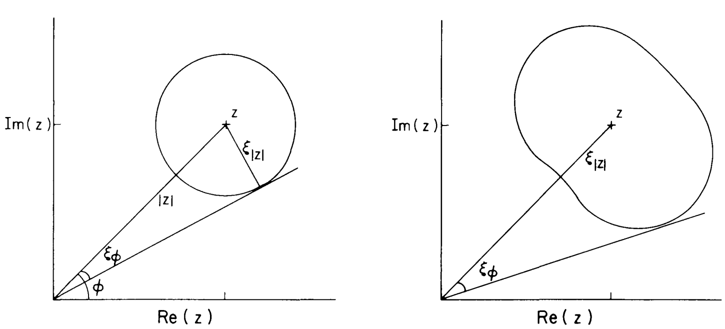

Fig. 2. Two types of error structure for an estimated impedance: *a* the error in apparent resistivity and impedance phase are of equal equivalent magnitude; *b* there is greater error in the impedance phase than in the apparent resistivity

Theory

Consider an n-layered earth in which one (or more) of the layers is vertically inhomogeneous, such that its conductivity varies linearly with depth (as illustrated in Fig. 3). In any layer, for a time-harmonic plane wave source, the horizontal electric field within the layer obeys the well-known diffusion equation (dependence of the electromagnetic fields on frequency is assumed throughout)

$$\frac{d^2}{dz^2} E_x(z) - i\omega\mu\sigma(z)\, E_x(z) = 0 \tag{1}$$

where ω is the angular frequency of the incident source, μ is the magnetic permeability of the medium, and $\sigma(z)$ is its conductivity as a function of depth z.

For layers of constant conductivity, i.e. $\sigma(z) = \sigma_j$ for $z_{j-1} \leqq z \leqq z_j$, the solution to equation (1) is simply

$$E_x(z) = A_j \exp(-k_j(z - z_{j-1})) + B_j \exp(k_j(z - z_{j-1})) \tag{2a}$$

where z_{j-1} is the depth to the bottom of the $(j-1)$'th layer (i.e. the top of the j'th layer), $k_j = \sqrt{i\omega\mu_j\sigma_j}$, and A_j and B_j are the layer constants. The magnetic field within this layer can be determined by application of the relation $dE_x(z)/dz = -i\omega\mu_j H_y(z)$ to yield

$$H_y(z) = \frac{k_j}{i\omega\mu_j}\left[A_j \exp(-k_j(z - z_{j-1})) - B_j \exp(k_j(z - z_{j-1}))\right]. \tag{2b}$$

For a layer in which the conductivity varies linearly with depth, the conductivity function at depth z, $\sigma(z)$ is given by

$$\sigma(z) = \sigma_j^t + \alpha_j(z - z_{j-1}) \tag{3}$$

with the conductivity gradient defined as

$$\alpha_j = \frac{\sigma_j^b - \sigma_j^t}{h_j}$$

where σ_j^t and σ_j^b denote the conductivities at the top and bottom of the j'th layer respectively, and h_j is the layer's thickness, hence $h_j = z_j - z_{j-1}$. It can be shown (Kao 1981, 1982; Kao and Rankin, 1980) that the horizontal electric field within this layer obeys the Airy differential equation

$$\frac{d^2}{d\eta_j^2} E_x(z) - \eta_j E_x(z) = 0 \tag{4}$$

where

$$\eta_j = \beta_j[\sigma_j^t + \alpha_j(z - z_{j-1})] \tag{5}$$

with

$$\beta_j = \left(\frac{i\omega\mu_j}{\alpha_j^2}\right)^{1/3}$$

and the root with phase of $\pi/6$ being chosen for β_j. (This assures that the Airy function Ai decays to zero at infinite depth.)

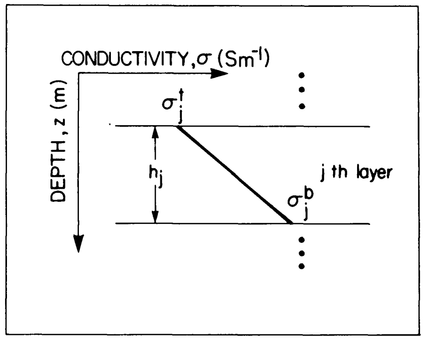

Fig. 3. A parameterization of a layer that has a linear gradient in conductivity with depth

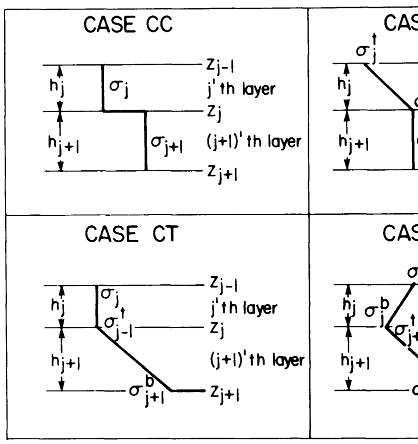

Fig. 4. The four possible layer interface cases. C denotes a layer in which the conductivity is a constant; T denotes one with a gradient in conductivity. In each case, the first letter denotes the upper layer

The solution to Eq. (4) can be expressed in terms of Airy functions of the first and second kinds (Abramowitz and Stegun, 1970), viz.

$$E_x(z) = A_j \mathrm{Ai}(\eta_j) + B_j \mathrm{Bi}(\eta_j) \tag{6a}$$

where Ai and Bi are the Airy functions. As before, the magnetic field is given by the derivative of $E_x(z)$ with respect to z, divided by $-i\omega\mu_j$, viz.

$$H_y(z) = \frac{-\eta_j'}{i\omega\mu_j}[A_j \mathrm{Ai}'(\eta_j) + B_j \mathrm{Bi}'(\eta_j)] \tag{6b}$$

where the prime denotes differentiation with respect to depth, and hence $\eta_j' = (i\omega\mu_j/\alpha_j^2)^{1/3}\alpha_j$. Note that it is not possible to simplify the expression for η_j' to $(i\omega\mu_j\alpha_j)^{1/3}$ because α_j can take negative values and we always take the root of β_j with phase $\pi/6$.

Using the appropriate boundary conditions at the interface between the j'th and the $(j+1)$'th layers, the coefficients A_j and B_j can be expressed in terms of the coefficients A_{j+1} and B_{j+1}. This relation between successive layer constants can be utilized to build up a solution matrix by combining all the individual layer connection matrices. For the final compounded solution matrix, there are $2n$ unknowns (the A_j's and B_j's for $j = 1, n$) but only $2n-2$ boundary conditions (two on each of the $n-1$ interfaces). This difficulty is overcome by noting that $B_n=0$, i.e. no upward propagating wave is permitted from the lower half-space (which may, or may not, have $\alpha_n=0$ but must not be less than zero), and by normalizing the layer constants by setting $A_n=1$. The complex impedance at any point within the earth is then simply calculated in terms of the ratio of the horizontal electric to magnetic fields, viz.

$$Z(z)=\frac{E_x(z)}{H_y(z)} \tag{7}$$

from which the magnetotelluric apparent resistivity and impedance phase functions are derived by

$$\rho_a(z)=\frac{1}{\omega\mu_0}|Z(z)|^2 \quad \text{and} \quad \phi(z)=\tan^{-1}(\operatorname{Im} Z(z)/\operatorname{Re} Z(z)).$$

In order to accommodate any model configuration, it is necessary to evaluate the boundary conditions for four separate cases, as illustrated in Fig. 4. Note that it is not possible to derive the fully general solution involving Airy functions alone because of the computational restrictions for the case when $\alpha_j=0$, i.e., the j'th layer has a constant conductivity. Associating the letter C (constant) with a layer in which the conductivity is constant, and T (transitional) with a layer in which there is a gradient in conductivity, the four possible interface combinations are CC, TC, CT, and TT. The layer connection matrices for the four cases are detailed below.

Case CC: $\alpha_j=\alpha_{j+1}=0$

$$\begin{pmatrix} e^{-k_jh_j} & e^{k_jh_j} & -1 & -1 \\ e^{-k_jh_j} & -e^{k_jh_j} & \dfrac{-k_{j+1}}{k_j} & \dfrac{k_{j+1}}{k_j} \end{pmatrix}. \tag{8a}$$

Case TC: $\alpha_j \neq \alpha_{j+1}=0$

$$\begin{pmatrix} \mathrm{Ai}(\beta_j\sigma_j^b) & \mathrm{Bi}(\beta_j\sigma_j^b) & -1 & -1 \\ \mathrm{Ai}'(\beta_j\sigma_j^b) & \mathrm{Bi}'(\beta_j\sigma_j^b) & \dfrac{k_{j+1}}{\eta_j} & \dfrac{-k_{j+1}}{\eta_j'} \end{pmatrix}. \tag{8b}$$

Case CT: $\alpha_j=0 \neq \alpha_{j+1}$

$$\begin{pmatrix} e^{-k_jh_j} & e^{k_jh_j} & -\mathrm{Ai}(\beta_{j+1}\sigma_{j+1}^t) & -\mathrm{Bi}(\beta_{j+1}\sigma_{j+1}^t) \\ e^{-k_jh_j} & -e^{k_jh_j} & \dfrac{\eta_{j+1}'}{k_j}\mathrm{Ai}'(\beta_{j+1}\sigma_{j+1}^t) & \dfrac{\eta_{j+1}'}{k_j}\mathrm{Bi}'(\beta_{j+1}\sigma_{j+1}^t) \end{pmatrix} \tag{8c}$$

Case TT: $\alpha_j \neq \alpha_{j+1} \neq 0$

$$\begin{pmatrix} \mathrm{Ai}(\beta_j\sigma_j^b) & \mathrm{Bi}(\beta_j\sigma_j^b) & -\mathrm{Ai}(\beta_{j+1}\sigma_{j+1}^t) & -\mathrm{Bi}(\beta_{j+1}\sigma_{j+1}^t) \\ \mathrm{Ai}'(\beta_j\sigma_j^b) & \mathrm{Bi}'(\beta_j\sigma_j^b) & -\dfrac{\eta_{j+1}'}{\eta_j'}\mathrm{Ai}'(\beta_{j+1}\sigma_{j+1}^t) & -\dfrac{\eta_{j+1}'}{\eta_j'}\mathrm{Bi}'(\beta_{j+1}\sigma_{j+1}^t) \end{pmatrix} \tag{8d}$$

where superscripts t and b refer to top and bottom respectively (see Fig. 3).

Hence, given any one of the four cases, the coefficients A_j and B_j can easily be computed in terms of A_{j+1} and B_{j+1}. Note that it is not required that $\sigma(z)$ be continuous across CT, TC, or TT type interfaces. There can be a discontinuity in conductivity at all four types of interface, such that $\sigma_j^b \neq \sigma_{j+1}^t$.

As an example, for a two-layer earth in which the top layer is a transition zone and the half-space is of constant conductivity, then the solution matrix is given by the single connection matrix for case TC (Eq. (8b)). Hence, the relation between the layer constants is given by

$$\begin{pmatrix} \mathrm{Ai}(\beta_1\sigma_1^b) & \mathrm{Bi}(\beta_1\sigma_1^b) & -1 & -1 \\ \mathrm{Ai}'(\beta_1\sigma_1^b) & \mathrm{Bi}'(\beta_1\sigma_1^b) & \dfrac{k_2}{\eta_1'} & \dfrac{-k_2}{\eta_1'} \end{pmatrix} \begin{pmatrix} A_1 \\ B_1 \\ 1 \\ 0 \end{pmatrix} = \begin{pmatrix} 0 \\ 0 \end{pmatrix}. \tag{9}$$

For a three-layered earth, as considered in detail by Kao (1981, 1982) and Kao and Rankin (1980), with a top layer of type C, a middle layer of type T, and a type C half-space, i.e. a total model descriptor of CTC, then the solution matrix is

$$\begin{pmatrix} e^{-k_1h_1} & e^{k_1h_1} & -\mathrm{Ai}(\beta_2\sigma_2^t) & -\mathrm{Bi}(\beta_2\sigma_2^t) & 0 & 0 \\ e^{-k_1h_1} & -e^{k_1h_1} & \dfrac{\eta_2'}{k_1}\mathrm{Ai}'(\beta_2\sigma_2^t) & \dfrac{\eta_2'}{k_1}\mathrm{Bi}'(\beta_2\sigma_2^t) & 0 & 0 \\ 0 & 0 & \mathrm{Ai}(\beta_2\sigma_2^b) & \mathrm{Bi}(\beta_2\sigma_2^b) & -1 & -1 \\ 0 & 0 & \mathrm{Ai}'(\beta_2\sigma_2^b) & \mathrm{Bi}'(\beta_2\sigma_2^b) & \dfrac{k_3}{\eta_2'} & \dfrac{-k_3}{\eta_2'} \end{pmatrix} \begin{pmatrix} A_1 \\ B_1 \\ A_2 \\ B_2 \\ 1 \\ 0 \end{pmatrix} = \begin{pmatrix} 0 \\ 0 \\ 0 \\ 0 \end{pmatrix}. \tag{10}$$

Any arbitrary solution matrix can be built up in a similar fashion from the individual $n-1$ layer connection matrices given by Eq. (8a)–(8d). An illustration of the form of such a solution matrix is given in Fig. 5, where the crosses refer to elements, the values of which depend on the type of interface involved. The matrix

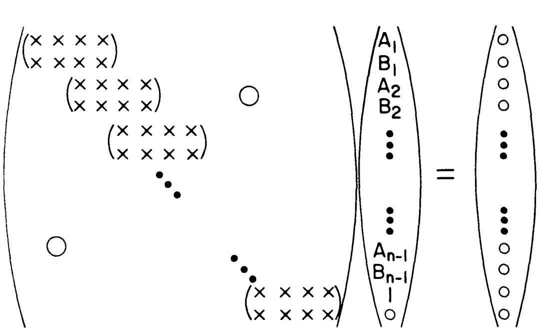

Fig. 5. The form of the general solution matrix for n layers. Each $\times$ denotes an element, whilst each sub-matrix denotes one of the layer connection matrices. Note that $A_n=1$ (arbitrary normalizing of the layer constants) and $B_n=0$ (no upward travelling wave permitted from the half-space)

has the property of being extremely sparse for large n, and therefore can be solved very efficiently. The solution matrix can be made upper triangular in $4n$ operations, and then solved by back substitution. Hence, the number of operations is of $O(n)$ instead of $O(n^3)$. For the evaluation of the complex Airy functions, we used the technique described in Schulten et al. (1979). Note that since our arguments of the Airy functions are all $i^{1/3}$ times a constant, it is simple to decide which computational technique to employ as the arguments all lie along a line in the complex plane (see Schulten et al., 1979, for details).

Examples

Oceanic lithosphere/asthenosphere

As mentioned in the Introduction, there have been many experiments carried out on the sea-floor that have successfully identified the presence and location of an ELAS layer beneath various recording locations in both the Atlantic and Pacific oceans. There is a strong correlation between the depths to these conducting layers and the ages of the oceanic crust above them (Oldenburg, 1981; Filloux, 1980b). We consider, as a typical model for the oceanic lithosphere and asthenosphere, a superficial 20-km upper layer of resistivity 5 Ωm, underlain by a more resistive layer of 100 Ωm to a depth of 80 km, below which is a half-space of 5 Ωm (see Fig. 6). This model has been taken from the interpretation of data recorded at MODE Station 5 in the Atlantic near Bermuda by Cox et al. (1980). The theoretical response of this model in the period range 0.1–10.0 cph (360–36,000 s) is illustrated in Fig. 7 (*solid* line).

If we assume that the error structure of the estimated response function is such that, at any frequency, it describes a circle in the complex impendance plane of radius ε_z (see Fig. 2a), then a 10% error in $|\hat{Z}|$ (which is approximately equal to a 20% error in ρ_a) is equivalent to a 6^0 error in ϕ_z. Assuming that with the most precise data possible the minimum standard errors achievable are 3.5% in ρ_a and 1^0 in ϕ, what minimum width would a transition zone need to be to be resolvable? Parameterizing the earth as *CCTC* in terms of (ρ_1, h_1) for layer 1, (ρ_2, h_2) for layer 2, (t_3) for layer 3 (the transition zone), and (ρ_4) for the half-space (see

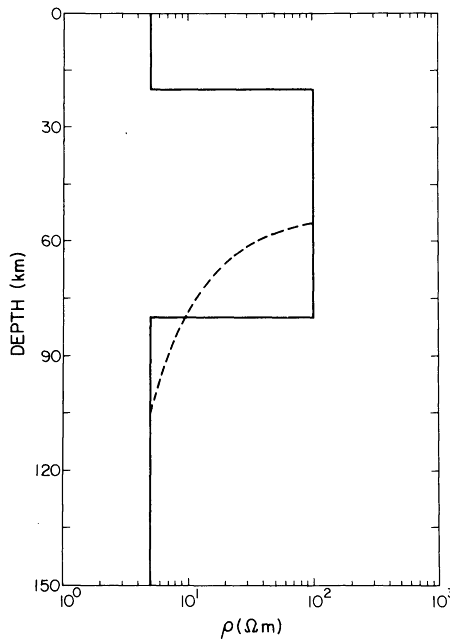

Fig. 6. The two models considered for the oceanic lithosphere/asthenosphere. The *dashed line* indicates a 50-km transition layer between the lithosphere and asthenosphere

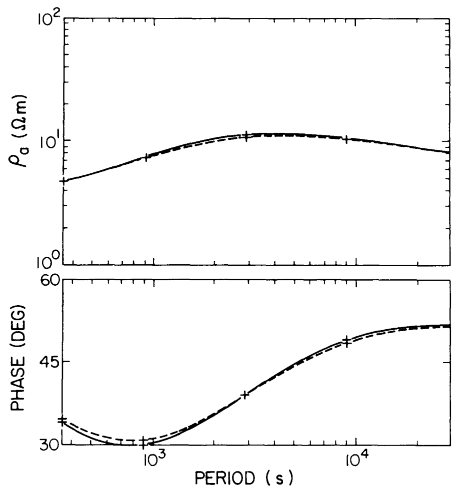

Fig. 7. The theoretical responses the two models illustrated in Fig. 6 in the period range of observation of a typical seafloor experiment. The *solid lines* are the response the model without a transition layer, whilst the *dashed lines* are the response the model with a 50-km transition layer, between the lithosphere and asthenosphere

Fig. 6), where h_2 is adjusted such that $h_1+h_2+t_3/2 = 80$ km (i.e. the centre of the transition zone occurs at the previous conductivity discontinuity between the "lithosphere" and "asthenosphere"), then t_3 must be at least 50 km to be detectable for the errors assigned. (Note that we have assumed no discontinuity in conductivity at the top and bottom of the transition zone.) For such a model, the surface response of which is illustrated in Fig. 7, the maximum difference in the responses between it and a model without a transition zone is 3.5% in ρ_a at a period of 4,200 s, and 1^0 in ϕ at 800 s – both of which occur at the maximum and minimum in ρ_a and ϕ respectively. From the apparent resistivity data alone, the resolution of t_3, i.e. the value of the appropriate element along the diagonal of the resolution matrix, is only 0.56. For the phase data alone, the resolution of this model parameter is 0.76, and combining the two, i.e. inverting the apparent resistivity and phase data simultaneously, this value is 0.99. In terms of model parameter ordering, t_3 is the most important parameter for the phase data, i.e. it has the largest contribution in the best-resolved mixed model parameter (given by the first row of the parameter eigenvector matrix). For ρ_a data alone, t_3 is classed as *marginally important*, as the standard error associated with it is of the order of 30%. The worst-resolved parameter of the model is ρ_2, the resistivity of the lithosphere (this was noted by Cox et al., 1980). However, even though t_3 appears to be well resolved, given sufficiently accurate data, it displays a high correlation (>0.95) with parameters h_2 and ρ_4. Hence, by varying h_2 and ρ_4 appropriately, it may be possible to find a model without a transition zone that satisfies the data to within the statistical error.

Thus, it appears to be an extremely difficult task requiring highly precise phase data to identify a transition zone between the lower lithosphere and asthenosphere for this oceanic model. This is because the lithosphere is virtually "invisible" to electromagnetic fields due to it being between two conducting layers.

Continental lithosphere/asthenosphere

The model taken for the continental lithosphere/asthenosphere is the three-layer model presented by Jones (1982a) for northern Sweden, which is illustrated in Fig. 1a. For a theoretical response in the period range 10–10^4 s with standard errors of 3.5% on ρ_a and 1^0 on ϕ, the model parameter t_3 (see Fig. 1c) becomes an important model parameter for ρ_a data alone when it exceeds 40 km. For the phase data, however, t_3 becomes an important parameter when it is greater than 30 km. At this thickness, the error in $\log(t_3)$ is 100% for ρ_a data alone, 80% for ϕ data alone, and 20% if both ρ_a and ϕ are inverted together.

Considering real data, Fig. 8 displays the apparent resistivity and impedance phase estimates, with their standard errors, for northern Scandinavia (Kiruna), determined using the horizontal spatial gradient technique Jones (1980). Also illustrated in the figure is the response of the best-fitting three-layer model (Fig. 1a). The minimum thickness of t_3 which causes at least one of the theoretical responses to exceed the error bounds is 50 km (see Fig. 1c), the response of which is also shown in Fig. 8. Undertaking an SVD analysis of the model with the transition zone (Fig. 1c) and the data (see Jones, 1982a, and Ilkisik and Jones, 1984, for details), with the *a priori* constraint that $\rho_1 = 10^4\ \Omega$m (from the audiomagnetotelluric data of Westerlund, 1972), gives the singular values (Λ) and parameter eigenvector matrices (**V**) listed in Table 1. The singular values have all been normalized such that a value of 1 implies 100% standard error in that particular eigenparameter. The three tables are for the cases when there exists (i) ρ_a data alone, (ii) ϕ data alone, and (iii) both ρ_a and ϕ data. The model parameter that has the largest contribution in the best resolved eigenparameter

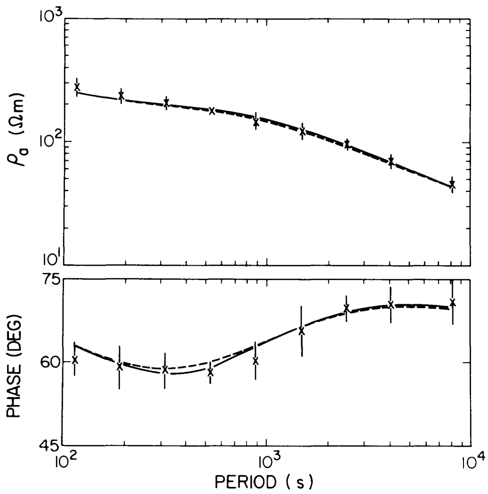

Fig. 8. The Kiruna data derived by Jones (1980) together with their standard errors. Also shown are the theoretical responses to the two models illustrated in Fig. 1a, c. The *solid lines* are the response to the model without a transition layer, whilst the *dashed lines* are the response to the model with a 50-km transition, between the lithosphere and asthenosphere

Table 1. Singular values, parameter eigenvectors, and their variances for the Kiruna data illustrated in Fig. 8 and the model in Fig. 1c

v_i	H_1	R_2	H_2	T_3	R_4	λ_i
RHO matrix — i.e. $\rho_a(f)$ data alone — $q^*=3.9$						
v_1	−0.45	−0.39	**−0.69**	0.39	−0.15	72
v_2	**0.59**	0.48	−0.50	0.11	−0.41	26
v_3	−0.27	−0.11	0.04	**−0.62**	**−0.73**	15
v_4	−0.03	−0.02	0.52	**0.67**	−0.53	1.5
v_5	0.62	−0.78	0.02	−0.06	−0.06	0.31
PHA matrix — i.e. $\phi(f)$ data alone — $q=2.7$						
v_1	−0.22	−0.04	−0.36	**0.87**	0.27	20
v_2	**0.85**	−0.10	−0.50	0.04	−0.12	8.0
v_3	−0.18	−0.29	−0.46	−0.46	−0.68	0.74
v_4	−0.25	0.75	−0.53	−0.18	−0.23	0.63
v_5	−0.36	−0.58	−0.36	−0.07	−0.63	0.02
TOT matrix — i.e. both $\rho_a(f)$ and $\phi(f)$ data — $q=4.9$						
v_1	−0.44	−0.37	**−0.68**	0.43	−0.13	73
v_2	**0.62**	0.45	−0.50	0.12	−0.38	26
v_3	−0.19	−0.19	−0.10	**−0.71**	−0.64	21
v_4	**0.53**	**−0.61**	−0.28	−0.31	0.41	6.6
v_5	0.32	−0.50	0.44	0.45	−0.51	2.5

* q denotes the rank of the Jacobian matrix, which is the number of resolved eigenparameters

for case (i) is h_2, with a standard error of less than 2%. The third eigenparameter for case (i) has a significant contribution from t_3, and is $t_3\rho_4$, with an associated standard error of 7%. Eigenparameter 4 is equivalent to t_3/ρ_4 ($=t_3\sigma_4$), and is a marginally important parameter as its standard error is 45%. For the phase data, however, case (ii), then the model parameter t_3 dominates the best-resolved eigenparameter, which has a standard error of 5%. For case (iii), then t_3 dominates the third eigenparameter, which has a standard error of 5%. (For comparison of the layered-earth type models, both with and without a transition zone

(Figs. 1c and 1a respectively), with an inversion of the Kiruna data in terms of a continuous $\sigma(z)$, Fig. 1b illustrates an acceptable C^{2+} model derived by Parker's (1980) scheme. The model is the one with the largest permissible σ_0 (0.05 Sm^{-1}) which is acceptable by the χ^2 statistic. Disregarding the geophysically untenable conducting top layer implied by the inversion, the model is in excellent agreement with the layered-earth models with regard to the position of the lithosphere/asthenosphere boundary and their respective resistivities. Parker's H^+ model for this data was also shown to be in agreement with the model illustrated in Fig. 1a (Jones, 1984).

Hence, given sufficiently precise phase data, it is possible to resolve parameter t_3 for a continental lithosphere/asthenosphere of the structure considered here. If there exists a lower crustal conducting layer, however, such as is true for the southern Finland region around Sauvamäki (Jones et al., 1983), then the upper mantle is between two zones of higher conductivity. In this case the most important parameter for the phase data is no longer the model parameter t_4 (the transition zone width between the third layer, i.e. the upper mantle of 100 Ωm and the asthenosphere), but is $S_2 = h_2/\rho_2$, i.e. the depth integrated conductivity of the conducting lower crustal layer. However, addition of phase data of 1^0 standard error to apparent resistivity data of standard error 3.5% increases the resolution of t_4 from 0.47 to 0.79.

Conclusions

In this paper, the work of Kao (1981, 1982) and Kao and Rankin (1980), for the case where a model contains layers with linear gradients in electrical conductivity with depth, has been generalized. We have shown how the solution matrix for an n-layered earth can be built up from $n-1$ layer connection matrices, which are given in Eq. (8a)–(8d) for the four possible cases. The solution matrix for n large is exceedingly sparse and accordingly can be solved very efficiently. The technique for solution involves forming an upper triangular matrix, and then back substituting, hence no "general" matrix inverse is undertaken.

It has been pointed out to us by an (unknown) referee that it is possible to derive a recursion relationship for Z_j in terms of Z_{j-1}, as in the uniform layer case. However, using the efficient matrix inversion technique described above leads to a solution for Z_j with the same accuracy and entailing the same order of number of operations as for a recursion relation solution. We prefer our solution matrix approach over a recursion relation for its mathematical elegance and its inherent simplicity in describing the physical relationships at the interfaces.

It would, of course, be possible to generate the response function of a transition layer by replacing the transition layer by a sufficient number of thin layers of constant conductivity and appropriate thicknesses. However, this approach is not satisfactory because (i) it is difficult to know the minimum number of thin layers, and their layer parameters, required (see the comments by Kao, 1982, on the work by Kao and Rankin, 1980), (ii) computation time is increased substantially, and (iii) an inversion of real data is made more difficult due to the increased number of model parameters.

We have applied the theory presented to the specific problem of determining if a transition zone in electrical conductivity can be resolved between the base of the lithosphere and the electrical asthenosphere – or ELAS layer. Using a singular value decomposition of the system matrix, the parameters for two particular models have been inspected for resolution.

For the model representing "young" oceanic lithosphere with an ELAS layer at 80 km, it is not possible to determine if a transition zone exists between the lithosphere and asthenosphere due to the existence of a highly conducting layer beneath the ocean, as interpreted by Cox et al. (1980). Even with highly accurate apparent resistivity and phase data, the transition zone has to be of such large magnitude compared to the depth of the ELAS layer as to be physically untenable. Accordingly, layered-earth models, in which the conductivity is constant within each layer, are satisfactory and adequate representations of the lithospher/asthenosphere boundary in this case.

For a continental lithosphere/asthenosphere where the conductivity is an increasing function with depth, given sufficiently precise data it has been shown that the width of a transition zone can be resolved. However, it is imperative that the phase data be as well determined as the apparent resistivity data. The best-resolved parameter of the phase data for the model considered (Fig. 1c) together with the responses observed (Fig. 8) is t_3, the thickness of the transition zone layer. However, it is often the case that the error structure is more like Fig. 2b than like Fig. 2a, and hence the model structure is resolved mostly by the apparent resistivity data. Accordingly, we wish to make the point strongly that workers be encouraged to attempt to derive more precise phase data.

Acknowledgements. One of the authors (AGJ) has received financial support from grants awarded to Professor G.D. Garland (NSERCC A2115) and to Professors R.N. Edwards and G.F. West (NSERCC G0501), for which he wishes to acknowledge his gratitude. TC would like to express his thanks to Drs. R.C. Bailey and R.N. Edwards for their support and informative discussions. Both authors are grateful to Dr. R.L. Parker for providing the coding of his inversion routine and to the (unknown) referee for many valuable comments on an earlier version of this manuscript.

References

Abramowitz, M., Stegun, I.A.: Handbook of mathematical functions. Dover, New York 1970

Ádám, A., Vanyan, L.L., Varlamov, D.A., Yegorov, I.V., Shilovski, A.P., Shilovski, P.P.: Depth of crustal conducting layer and asthenosphere in the Pannonian basin determined by magnetotellurics. Phys. Earth Planet. Inter **28**, 251–260, 1982

Chave, A.D., von Herzen, R.P., Poehls, K.A., Cox, C.S.: Electromagnetic induction fields in the deep ocean north-east of Hawaii: implications for mantle conductivity and source fields. Geophys. J.R. Astron. Soc. **66**, 379–406, 1981

Cox, C.S., Filloux, J.H., Gough, D.I., Larsen, J.C., Poehls, K.A., von Herzen, R.P., Winter, R.: Atlantic lithospheric sounding. In: Electromagnetic Induction in the Earth and Moon, U. Schmucker, ed.: pp 13–32. Centr. Acad. Publ. Japan, Tokio and D. Reidel Publ. Co., Dordrecht 1980

Edwards, R.N., Bailey, R.C., Garland, G.D.: Conductivity anomalies: lower crust or asthenosphere? Phys. Earth Planet. Inter. **25**, 263–272, 1981

Filloux, J.H.: North Pacific magnetotelluric experiments. In: Electromagnetic Induction in the Earth and Moon, U. Schmucker, ed.: pp 33–43. Centr. Acad. Publ. Japan, Tokio and D. Reidel Publ. Co., Dordrecht 1980a

Filloux, J.H.: Magnetotelluric soundings over the northeast Pacific may reveal spatial dependence and conductance of the asthenosphere. Earth Planet. Sci. Lett. **46**, 244–252, 1980b

Filloux, J.H.: Magnetotelluric exploration of the north Pacific: progress report and prelimenary soundings near a spreading ridge. Phys. Earth Planet. Inter. **25**, 187–195, 1981

Fischer, G., Schnegg, P.-A.: The dispersion relations of the magnetotelluric response and their incidence on the inversion problem. Geophys. J.R. Astron. Soc. **62**, 661–673, 1980

Ilkisik, O.M., Jones, A.G.: Statistical evaluation of MT and AMT methods applied to a basalt covered area in southeastern Anastolia, Turkey. Geophys. Prospect., in press 1984

Inman, J.R.: Resistivity inversion with ridge regression. Geophysics **40**, 798–817, 1975

Jones, A.G.: Geomagnetic induction studies in Scandinavia – I. Determination of the inductive response function from the magnetometer data. J. Geophys. **48**, 181–194, 1980

Jones, A.G.: On the electrical crust-mantle structure in Fennoscandia: no Moho and the asthenosphere revealed? Geophys. J.R. Astron. Soc. **68**, 371–388, 1982a

Jones, A.G.: Observations of the electrical asthenosphere beneath Scandinavia. Tectonophysics **90**, 37–55, 1982b

Jones, A.G.: The electrical structure of the lithosphere and asthenosphere beneath the Fennoscandian shield. J. Geomagn. Geoelectr., in press 1984

Jones, A.G., Olafsdottir, B., Tiikkainen, J.: Geomagnetic induction studies in Scandinavia – III. Magnetotelluric observations. J. Geophys. **54**, 35–50, 1983

Kao, D.: Magnetotelluric response on vertically inhomogeneous earth. J. Geophys. Res. **86**, 3027–3038, 1981

Kao, D.: Magnetotelluric response on vertically inhomogeneous earth having conductivity varying linearly with depth. Geophys. Prospect. **30**, 866–878, 1982

Kao, D., Rankin, D.: Magnetotelluric response on inhomogeneous layered earth. Geophysics **45**, 1793–1802, 1980

Krasnobayeva, A.C., D'Yakonov, B.P., Astaf'Yev, P.F., Batalova, O.V., Vishnev, V.S., Gavrilova, I.E., Zhuravleva, P.B., Kirillov, S.K.: Structure of the northeastern part of the Baltic shield based on magnetotelluric data. Izvestiya, Earth Phys. **17**, 439–444, 1981

Kurtz, R.D.: Magnetotelluric interpretation of crustal and mantle structure in the Grenville Province. Geophys. J.R. Astron. Soc. **70**, 373–397, 1982

Larsen, J.C.: Removal of local surface conductivity effects from low frequency mantle response curves. Acta Geodaet., Geophys. et Montanist. Acad. Sci. Hung. **12**, 183–186, 1977

Lawson, C.L., Hanson, R.J.: Solving least-squares problems. Prentice-Hall, New Jersey, ISBN 0-13-822585-0, 1974

Oldenburg, D.W.: Conductivity structure of oceanic upper mantle beneath the Pacific plate. Geophys. J.R. Astron. Soc. **65**, 359–394, 1981

Parker, R.L.: The inverse problem of electromagnetic induction: existence and construction of solutions based on incomplete data. J. Geophys. Res. **85**, 4421–4425, 1980

Schmucker, U.: Status report on the Project ELAS. IAGA News **20**, 62–72, 1981

Schmucker, U.: Reports on an informal meeting of the Project ELAS. IAGA News **21**, 89–90, 1982

Schulten, Z., Anderson, D.G.M., Gordon, R.G.: An algorithm for the evaluation of the complex Airy functions. J. Comp. Phys. **31**, 60–75, 1979

Vanyan, L.L.: Progress report on ELAS-Project. IAGA News **19**, 73–84, 1980

Weidelt, P.: The inverse problem of geomagnetic induction. Z. Geophys **38**, 257–289, 1972

Westerlund, S.: Magnetotelluric experiments in the frequency range 0.01 Hz to 10 kHz. KGO Report, 72:10, Kiruna Geophysical Observatory, 1972

Wiggins, R.A.: The general linear inverse problem: implications of surface waves and free oscillations for Earth structure. Rev. Geophys. Space. Phys. **10**, 251–285, 1972

Received December 1, 1983; Revised version March 21, 1984
Accepted March 22, 1984